

Density functional theory calculation of crystal-field energy levels for Yb^{3+} in the $\text{Cs}_2\text{NaYbF}_6$ crystal

Lixin Ning and Gian Paolo Brivio

Dipartimento di Scienza dei Materiali and CNISM, Università degli Studi di Milano-Bicocca, via Cozzi 53, 20125 Milano, Italy

(Received 3 January 2007; revised manuscript received 22 March 2007; published 29 June 2007)

We present calculations of the crystal-field (CF) parameters for Yb^{3+} in $\text{Cs}_2\text{NaYbF}_6$ by means of the density functional theory (DFT). The CF parameters are evaluated from the CF potential constructed from the DFT calculations on the $[\text{YbF}_6]^{3-}$ system with the $4f$ electrons of Yb^{3+} frozen into the effective core potential. A repulsive pseudopotential without any free parameters is introduced to account for the nonorthogonality between the $4f$ all-electron orbitals and the DFT-valence orbitals. From the derived CF parameters, the Yb^{3+} energy levels are calculated on the basis of the crystal-field theory. Good agreement with experiments is obtained. The derived parameters are discussed in terms of overlap, covalency, and exchange contributions, respectively. The numerical accuracy of the calculation is finally addressed.

DOI: [10.1103/PhysRevB.75.235126](https://doi.org/10.1103/PhysRevB.75.235126)

PACS number(s): 71.70.Ch, 31.15.Ar, 31.15.Ew

I. INTRODUCTION

Optical properties of materials containing lanthanide ions have been intensively studied in several scientific domains, ranging from laser physics to molecular biology.¹ The performances of these materials are mainly determined by the electronic energy-level structure of the lanthanide ions. For the ground $4f^N$ electronic configurations, the splitting of energy levels is caused by the atomic interactions of the $4f$ electrons (e.g., the Coulomb and the spin-orbit interactions), and, to a less extent, by the crystal-field (CF) interaction between the $4f$ electrons and the environment. Because the $4f$ orbital is shielded from influence of the surroundings by the outer closed $5s^25p^6$ shells and thus exhibits a rather small overlap with the electron density of neighboring atoms, the $4f$ atomic interactions that yield the multiplet structure are mostly independent of change of the environment. On the other hand, the CF interaction that splits the multiplets into the CF energy levels is environment dependent. The correlation between the lanthanide environment and the CF energy-level structure allows for a fine-tuning of the electronic levels, making it possible to obtain a rational design of lanthanide-based devices with predetermined optical functions.

The electronic energy levels of the highly localized $4f^N$ configurations have been successfully modeled by the conventional crystal-field theory (CFT).¹ The theory introduces adjustable energy parameters for the atomic and CF interactions. For the CF interaction, the number of parameters is determined by the site symmetry of the lanthanide ion, and their values are obtained by fitting to the experimental CF energy levels deduced from the observed electronic spectra with high resolution. However, when the complexity of the lanthanide local environment is increased or the site symmetry is low (e.g., in amorphous systems), the number of CF parameters will most probably exceed the number of observables that can be derived from experiments. In these cases, computational models free of adjustable parameters for the CF interaction would be necessary.

First-principles calculations of the electronic structure of systems containing the lanthanide $4f$ orbitals are still a con-

siderable challenge due to the extremely complex electronic structure of the $4f$ elements, the large relativistic effects, and the strong correlation. Despite these difficulties, the *ab initio* pseudopotential method has proven to be one of the most successful approaches. Dolg *et al.*² examined the split levels of lanthanide monoxides and monofluorides by a combination of the quasirelativistic pseudopotential and the CF calculations, where the $4f$ shell was treated as a part of the lanthanide core. The CF parameters B_0^k ($k=2,4,6$) were determined by the difference between the matrix elements $\langle 4f, m | V | 4f, m \rangle$ ($m=0, \pm 1, \pm 2, \pm 3$), V being the electrostatic potential. Since the B_0^k values are less than 1% of the absolute values of the above matrix elements, small numerical accuracies in the integration schemes led to significant errors in the final results. Additional errors were introduced by neglecting the orthogonal requirement between the $4f$ all-electron orbitals and the valence electron orbitals.

In recent years, the density functional theory (DFT) has been used not only to predict ground-state properties (e.g., bond energy and molecular geometry) of lanthanide compounds but also to study their electronic structures, and good agreements with experiments have been obtained.³⁻⁷ Because the DFT is not directly applicable to the study of the excited states, it is usually combined with the CFT to calculate the electronic structure of lanthanide ions. In such calculations, the charge density of the compound obtained from the DFT calculations is usually employed to construct the CF potential, from which the CF parameters are calculated. Using the diatomic molecules LnF as models ($\text{Ln}=\text{Ce}$ to Yb), Dai and co-workers^{3,4} have shown that the energy levels of lanthanide ions can be calculated reasonably well by constructing the CF potential directly from the DFT-generated effective potential. They introduced pseudopotentials to account for the Pauli repulsion involving the $4f$ electrons (which were treated as valence electrons in their DFT calculations) when calculating the parameters from the constructed CF potential. Three adjustable parameters were included in the expressions of the pseudopotentials. Their values were determined by fitting the calculated CF levels to experiments and were considered to be more transferable than the usual CF parameters. A scheme to improve their method by construct-

ing the CF potential with the $4f$ electrons frozen in the lanthanide core has also been proposed.

In this paper, we report calculations of the CF parameters, and hence of the CF energy levels, by a combination of the hybrid DFT with the conventional CFT. The $4f$ shell has been included into the lanthanide core. The DFT-generated charge densities are then used to construct a repulsive pseudopotential to account for the nonorthogonality between the $4f$ all-electron orbitals and the DFT-valence orbitals when calculating the CF parameters by a perturbation. No adjustable parameter has been used. The *ab initio* CF potential constructed by the DFT is then used to calculate the CF parameters through numerical integration over a fine grid mesh of points. The ionic $\text{Cs}_2\text{NaYbF}_6$ crystal has been chosen for our investigation. The Yb^{3+} ion is located at the end of the lanthanide series with pronounced core character of the $4f$ electrons. This ion is commonly used as a sensitizer in Er^{3+} lasers because it has a much larger absorption cross section near 980 nm than Er^{3+} , and it efficiently transfers its excited state energy to the upper level of the Er^{3+} 1.5 μm transition. The $\text{Cs}_2\text{NaLnF}_6$ crystals are technologically interesting because they are harder and less moisture sensitive than the usual crystals. From a theoretical viewpoint these systems produce a tough test for the CF energy-level calculations since only two CF parameters are required for the $[\text{LnF}_6]^{3-}$ octahedral systems. Finally, well-defined experimental CF energy levels are available for the $\text{Cs}_2\text{NaYbF}_6$ crystal.⁸

This paper is organized as follows. A brief description of the CF parameter calculations is outlined in Sec. II A, while the derivation of the CF potential from the DFT calculations is given in Sec. II B. The details of the DFT calculations on $\text{Cs}_2\text{NaYbF}_6$ are presented in Sec. III. In Sec. IV, results of the calculation are tabulated and discussed, with the final conclusions collected in Sec. V.

II. THEORY

A. Evaluation of the crystal-field parameters

The Hamiltonian for the $4f^N$ electronic configuration of lanthanide ions in crystals may be written as

$$\mathbf{H} = \mathbf{H}_0 + \mathbf{H}_C + \mathbf{H}_{\text{SO}} + \mathbf{V}_{\text{CF}}, \quad (1)$$

where \mathbf{H}_0 , \mathbf{H}_C , and \mathbf{H}_{SO} are atomic Hamiltonians representing, respectively, the sum of the kinetic and potential energies of the $4f$ electrons in the field of the ion core, the Coulomb interaction between the $4f$ electrons, and the $4f$ spin-orbit interaction; see Ref. 1 for details. \mathbf{V}_{CF} is the CF Hamiltonian representing the interaction of the $4f$ electrons with the surroundings. This interaction is generally considered as a perturbation to the $4f$ electronic structure and can be written as⁹

$$\mathbf{V}_{\text{CF}}(\mathbf{r}) = \sum_{k=0}^{\infty} \sum_{q=-k}^k \mathbf{B}_q^k(r) \mathbf{C}_q^k(\theta, \varphi), \quad (2)$$

where the radial part is denoted by $\mathbf{B}_q^k(r)$ and the angular part by spherical tensor operators $\mathbf{C}_q^k(\theta, \varphi)$, which are related to spherical harmonic functions by

$$\mathbf{C}_q^k(\theta, \varphi) = \sqrt{\frac{4\pi}{2k+1}} Y_q^k(\theta, \varphi). \quad (3)$$

For convenience, it is assumed that the center of the coordinate system is on the lanthanide ion.

In the phenomenological approach to the CFT, the CF interaction \mathbf{V}_{CF} is parametrized in such a way that the radial part in Eq. (2) is replaced by the CF parameters B_q^k that are defined as

$$B_q^k = \langle R_{4f}(r) | \mathbf{B}_q^k(r) | R_{4f}(r) \rangle, \quad (4)$$

where $R_{4f}(r)$ is the $4f$ radial wave function. These CF parameters, together with the parameters for other atomic interactions, are usually determined by fitting the calculated CF energy levels to experimental ones, in which the energy levels are calculated by diagonalization of the total parametrized Hamiltonians. Once the optimized parameters are obtained, the energy-level structure of the lanthanide ion in the crystal can be constructed by using the standard CF calculations.¹

Given that the CF potential $\mathbf{V}_{\text{CF}}(\mathbf{r})$ can be determined *ab initio* (as shown in this work), the B_q^k parameters may be calculated by combining Eqs. (2)–(4):

$$\begin{aligned} B_q^k &= \langle R_{4f}(r) | \mathbf{B}_q^k(r) | R_{4f}(r) \rangle \\ &= \frac{2k+1}{4\pi} \int R_{4f}^2(r) \mathbf{C}_q^{k*}(\theta, \varphi) V_{\text{CF}}(r, \theta, \varphi) r^2 dr \sin \theta d\theta d\varphi, \end{aligned} \quad (5)$$

where use has been made of the orthonormal property of spherical harmonic functions:

$$\int Y_q^{k*}(\theta, \varphi) Y_{q'}^k(\theta, \varphi) \sin \theta d\theta d\varphi = \delta_{kk'} \delta_{qq'}. \quad (6)$$

In order to perform numerical integration, Eq. (5) is rewritten as

$$B_q^k = \frac{2k+1}{4\pi} \sum_i R_{4f}^2(r_i) \mathbf{C}_q^{k*}(\theta_i, \varphi_i) V_{\text{CF}}(r_i, \theta_i, \varphi_i) w_i, \quad (7)$$

where the summation is over the integration points (indicated by the symbol i) with the weighting factor w_i , which is proportional to the volume element represented by the points.

B. Construction of the crystal-field potential from the density functional theory

In the DFT,¹⁰ the electron density is written as a sum of single particle densities, and the variational method is used as a prescription for determining the ground-state energy and density. The correct electron density is given by the self-consistent solution of a set of single particle Schrödinger-like equations, known as the Kohn-Sham equations,

$$[\mathbf{T} + \mathbf{V}_{\text{el}}(\mathbf{r}) + \mathbf{V}_H(\mathbf{r}) + \mathbf{V}_{\text{XC}}(\mathbf{r})] \varphi_i(\mathbf{r}) = \varepsilon_i \varphi_i(\mathbf{r}), \quad (8)$$

and is expressed as a sum over the occupied orbitals,

$$\rho(\mathbf{r}) = \sum_{\text{OCC}} \varphi_i^*(\mathbf{r})\varphi_i(\mathbf{r}). \quad (9)$$

In the above two expressions, φ_i and ε_i are the single particle orbitals and the eigenvalues, respectively, \mathbf{T} is the noninteracting kinetic energy operator, \mathbf{V}_{ei} is the Coulomb potential due to the nuclei, \mathbf{V}_H is the Hartree potential, and \mathbf{V}_{XC} is the exchange-correlation potential. Both \mathbf{V}_H and \mathbf{V}_{XC} depend on ρ ,

$$\mathbf{V}_H(\mathbf{r}) = \int d\mathbf{r}' \frac{\rho(\mathbf{r}')}{|\mathbf{r} - \mathbf{r}'|} \quad (10)$$

and

$$\mathbf{V}_{\text{XC}}(\mathbf{r}) = \frac{\delta E_{\text{XC}}[\rho]}{\delta \rho(\mathbf{r})}. \quad (11)$$

Thus, the DFT effective potential [see Eq. (8)]

$$\mathbf{V}_{\text{eff}}(\mathbf{r}) = \mathbf{V}_{\text{ei}}(\mathbf{r}) + \mathbf{V}_H(\mathbf{r}) + \mathbf{V}_{\text{XC}}(\mathbf{r}) \quad (12)$$

is uniquely determined by the electron density $\rho(\mathbf{r})$ of the system.

The effective potential $\mathbf{V}_{\text{eff}}(\mathbf{r})$ generated by the DFT calculations on the lanthanide compound is used to construct the CF potential $\mathbf{V}_{\text{CF}}(\mathbf{r})$, from which the CF parameters B_q^k are calculated according to Eq. (7). Because $\mathbf{V}_{\text{CF}}(\mathbf{r})$ represents a potential acting on the $4f$ electrons of the lanthanide ion, the $4f$ contribution itself in the DFT-generated $\mathbf{V}_{\text{eff}}(\mathbf{r})$ needs to be excluded. This has been performed in Ref. 3 by removing the $4f$ electron density from $\rho(\mathbf{r})$ in Eq. (9) through modifying the relevant density matrix elements in the self-consistent effective potential $\mathbf{V}_{\text{eff}}(\mathbf{r})$. However, in the present work, the $4f$ orbitals were frozen into the lanthanide core during the self-consistent calculations using the effective core potential (ECP) for the lanthanide ion.² After the self-consistent calculations, it is usually difficult to separate out the ECP from the effective potential $\mathbf{V}_{\text{eff}}(\mathbf{r})$, due to the presence of its nonlocal (angular l -dependent) part. This part is to guarantee that the pseudovalence wave functions are orthogonal to the core states with the same angular momenta l . In combination with the ECP, the optimized $(7s6p3d)/[5s4p3d]$ Gaussian-type orbital valence basis set was used for the lanthanide ion. The resultant valence wave functions from this basis set experience the s , p , and d core potentials differently due to the different orthogonalizations. However, the f core potential is seen in the same way by all the l components of the valence wave functions since no f orbitals exist in the valence basis set. We may thus assume that the $4f$ core potential in $\mathbf{V}_{\text{eff}}(\mathbf{r})$ is mainly local and spherically symmetric.¹¹ Then, the summation in Eq. (12) can be recast in the following form:

$$\mathbf{V}_{\text{eff}}(\mathbf{r}) = \mathbf{V}_{\text{ECP}}^{4f}(\mathbf{r}) + \mathbf{V}'_{\text{eff}}(\mathbf{r}),$$

where the $4f$ core potential is denoted by $\mathbf{V}_{\text{ECP}}^{4f}(\mathbf{r})$. Substituting $\mathbf{V}_{\text{ECP}}^{4f}(\mathbf{r})$ for \mathbf{V}_{CF} into Eq. (5) yields

$$B_q^k = \frac{2k+1}{4\pi} \int R_{4f}^2(r) V_{\text{ECP}}^{4f}(r) r^2 dr \int \mathbf{C}_q^{k*}(\theta, \varphi) \sin \theta d\theta d\varphi,$$

where, according to Eq. (6), the angular integral part is zero unless $k=q=0$. As a consequence, the CF parameters B_q^k with $k \neq 0$, which are calculated from $\mathbf{V}_{\text{eff}}(\mathbf{r})$ and are also responsible for the CF splitting of energy levels, do not contain the $4f$ contributions. In this way, the complexities that would otherwise be involved in removing the $4f$ contribution in $\mathbf{V}_{\text{eff}}(\mathbf{r})$ are avoided.

To calculate the B_q^k parameters, a simple substitution of the effective potential $\mathbf{V}_{\text{eff}}(\mathbf{r})$ for the CF potential $\mathbf{V}_{\text{CF}}(\mathbf{r})$ is not sufficient. This is because the $4f$ all-electron orbital associated with the $R_{4f}(r)$ in Eq. (5), which is obtained from the relativistic Hartree-Fock calculations on the lanthanide ion, is not orthogonal to the DFT-valence orbitals, so that the tails of the $4f$ orbitals might reach the DFT-valence orbitals unphysically. To prevent such a situation, the $4f$ all-electron orbitals should be made orthogonal to the DFT-valence orbitals. Instead of orthogonalizing the orbitals, one can introduce a repulsive pseudopotential into the potential field felt by the $4f$ electrons to include the orthogonality condition. This method has been extensively studied by Szasz.¹² The pseudopotential keeps the $4f$ electrons out of the DFT-valence electrons, which is equivalent to the Pauli repulsion. In this work, we adopted a density-dependent pseudopotential expressed as¹²

$$\mathbf{V}_p(\mathbf{r}) = \frac{1}{2} (3\pi^2)^{2/3} \{ \rho^{2/3}(\mathbf{r}) - [\rho^{1/3}(\mathbf{r}) - \rho_0^{1/3}(\mathbf{r})]^2 \}, \quad (13)$$

where $\rho(\mathbf{r})$ is the electron density of the compound including the $4f$ core electrons and $\rho_0(\mathbf{r})$ is the valence electron density. Both electron densities are obtained by the DFT calculations along with $\mathbf{V}_{\text{eff}}(\mathbf{r})$. This form of pseudopotential has also been adopted by Dai and co-workers^{3,4} in the calculation of the CF parameters of lanthanide ions in diatomic molecules. They introduced adjustable parameters in the pseudopotential which were fitted to the experimental energy levels, as described in the Introduction. However, in the present calculation for Yb^{3+} in $\text{Cs}_2\text{NaYbF}_6$, no adjustable parameters have been introduced in Eq. (13). By adding the pseudopotential $\mathbf{V}_p(\mathbf{r})$ to $\mathbf{V}_{\text{eff}}(\mathbf{r})$, the *ab initio* CF potential is written as

$$\mathbf{V}_{\text{CF}}(\mathbf{r}) = \mathbf{V}_{\text{eff}}(\mathbf{r}) + \mathbf{V}_p(\mathbf{r}). \quad (14)$$

Then, by inserting the *ab initio* $\mathbf{V}_{\text{CF}}(\mathbf{r})$ in Eq. (7) with the all-electron $R_{4f}(r)$, the CF parameters can be calculated by numerical integration.

III. DETAILS OF THE DENSITY FUNCTIONAL THEORY CALCULATIONS

In the $\text{Cs}_2\text{NaYbF}_6$ crystal, the Yb^{3+} ion sits on the site of O_h symmetry with a first coordination shell of six F^- ions, as shown in Fig. 1. From a point-group consideration, only the CF parameters B_q^k with $k=4, 6$, and $q=0, \pm 4$ are nonzero with the relations

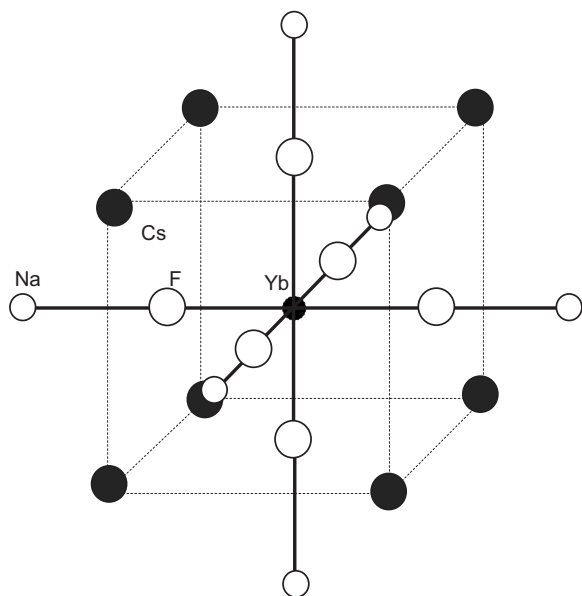


FIG. 1. Coordination environment of Yb^{3+} in the $\text{Cs}_2\text{NaYbF}_6$ crystal. Each Yb^{3+} is hexacoordinated to six F^- ions. The second coordination shell comprises eight Cs^+ ions at the corners of the cube. The third shell has six Na^+ ions occupying the vertices of the octahedron.

$$B_{\pm 4}^4 = (5/14)^{1/2} B_0^4 \quad \text{and} \quad B_{\pm 4}^6 = -(7/2)^{1/2} B_0^6. \quad (15)$$

For this ionic crystal, the $4f$ energy-level structure of Yb^{3+} ($4f^{13}$) depends almost totally on the $4f$ spin-orbit interaction (\mathbf{H}_{SO}) and the CF interaction (\mathbf{V}_{CF}) with the six nearest F^- ions. \mathbf{H}_{SO} leads to a splitting of the spectroscopic term 2F into the two multiplets ${}^2F_{7/2}$ and ${}^2F_{5/2}$, which are split by \mathbf{V}_{CF} into the CF energy levels. A schematic representation of the $4f$ energy-level splitting in $\text{Cs}_2\text{NaYbF}_6$ is presented in Fig. 2, where the CF energy levels are identified by irreducible representations Γ_i of the O_h point group. For the CF interaction \mathbf{V}_{CF} , the crystalline electrostatic potential from the rest of the crystal has been neglected, because it mainly affects the B_q^k parameters with $k=2$ which, however, do not exist for the O_h site symmetry. In fact, besides the single $[\text{YbF}_6]^{3-}$ cluster, we have performed DFT calculations on a much larger one including the ions up to the third coordination shell around Yb^{3+} (see Fig. 1) and also on the cluster $[\text{YbF}_6]^{3-}$ embedded in a background of 1434 point charges sitting on the crystallographic sites. The results are almost identical to those for the single $[\text{YbF}_6]^{3-}$ cluster; the differences are less than 1%. Therefore, in this paper, only the DFT study on the $[\text{YbF}_6]^{3-}$ cluster is reported. The experimental value of 2.482 Å for the Yb–F bond distance has been used.^{13,14}

The DFT calculations were performed by employing the hybrid B3LYP exchange-correlation functional^{15,16} as implemented in the GAUSSIAN 03 program.¹⁷ The 6–311G+(3df) basis set was employed for the F^- ions. For the lanthanide Yb^{3+} ion, the ECP of MWB59 by Dolg *et al.*^{18,19} and the related [5s4p3d]-GTO valence basis set were used. A total of $46+4f^{13}$ electrons are included in the lanthanide core and the remaining 11 electrons are treated explicitly.

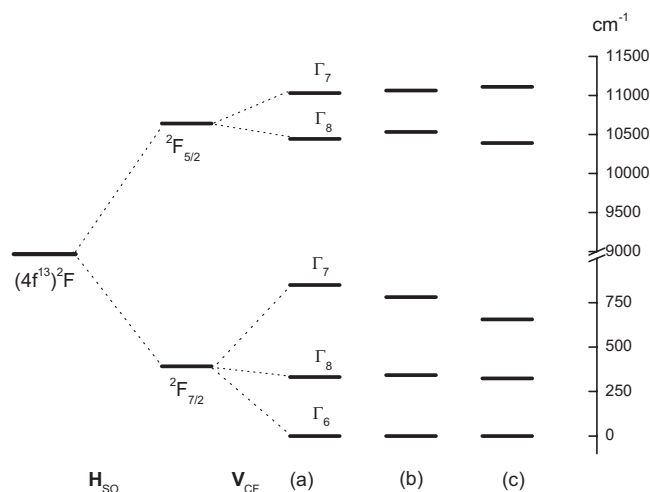


FIG. 2. (a) Schematic diagram of the Yb^{3+} ($4f^{13}$) energy levels in the $\text{Cs}_2\text{NaYbF}_6$ crystal showing the energy levels from the DFT calculations in this work. (b) gives the energy position of the levels obtained by fitting to the experimental energy levels. (c) shows the experimental energy levels. The energy values in (b) and (c) were taken from Ref. 8. Also presented is the splitting pattern of the $4f$ energy levels under the spin-orbit (H_{SO}) and CF (V_{CF}) interactions.

IV. RESULTS AND DISCUSSION

The electronic structure of $[\text{YbF}_6]^{3-}$ was first calculated by the DFT to obtain the effective potential $\mathbf{V}_{\text{eff}}(\mathbf{r})$ and the electron densities $\rho(\mathbf{r})$ and $\rho_0(\mathbf{r})$, from which the pseudopotential $\mathbf{V}_p(\mathbf{r})$ was generated according to Eq. (13). Then, from Eq. (14), the CF potential $\mathbf{V}_{\text{CF}}(\mathbf{r})$ was constructed and employed to calculate the CF parameters (i.e., B_0^4 and B_0^6) by Eq. (7). With these CF parameters and also that (ζ_{4f}) for the spin-orbit interaction, the CF energy levels were obtained by diagonalizing simultaneously the spin-orbit and CF Hamiltonians using the software LANTHANIDE.²⁰ The $4f$ radial wave function $R_{4f}(r)$ was obtained from the relativistic Hartree-Fock calculations.²¹ In Fig. 3, a schematic view on the $\mathbf{V}_{\text{eff}}(\mathbf{r})$, $\mathbf{V}_p(\mathbf{r})$, and $\mathbf{V}_{\text{CF}}(\mathbf{r})$ potentials along the Yb–F direction as a function of the distance r from the Yb^{3+} ion is presented as well as the squared $4f$ radial wave function $R_{4f}^2(r)$. In addition, the spin-orbit parameter ζ_{4f} was taken to be 2928 cm^{-1} in the calculations, which is the value for Yb^{3+} in the LaF_3 crystal.²²

Values of the B_0^4 and B_0^6 parameters obtained by the DFT calculations are listed in the fourth column (column “Total”) of Table I while the calculated energy levels are presented in the third column (column “DFT”) of Table II. Zhou *et al.*⁸ have performed an empirical fitting of the spin-orbit and CF parameters to the experimental energy levels of Yb^{3+} in $\text{Cs}_2\text{NaYbF}_6$. The fitted CF parameter values and the energy levels are listed in the last column of Table I and the fifth column of Table II, respectively. A schematic representation of the DFT-based, fitted, and experimental CF energy levels is shown in Fig. 2. From Table II and Fig. 2 one can see that the DFT-based energy levels agree overall very well with experiments. The agreement is surprisingly good in view of the fact that our use of the repulsive pseudopotential in Eq.

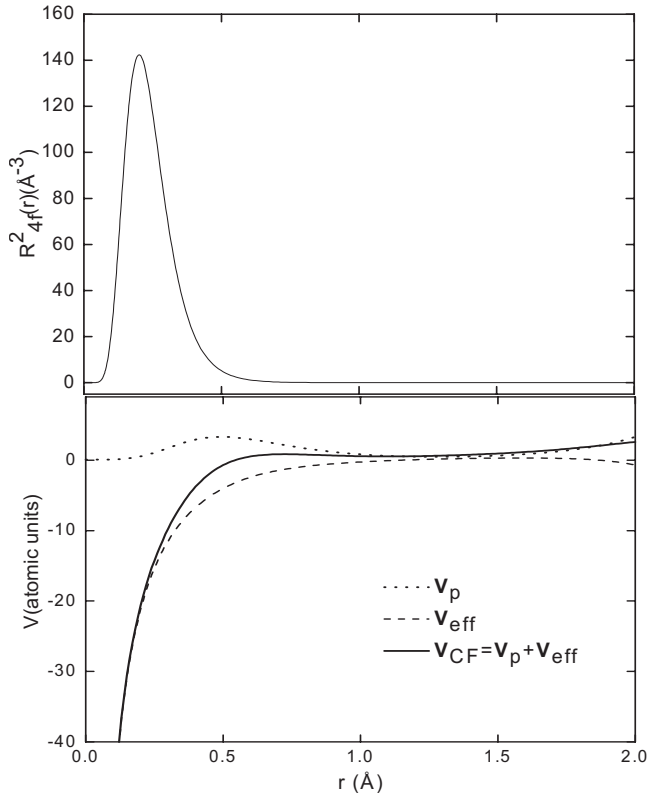


FIG. 3. Plots of the squared $4f$ radial wave function $R_{4f}^2(r)$ (upper part) and the various potentials generated by the DFT calculations (lower part) along the Yb-F direction as a function of the distance r from the Yb^{3+} ion.

(13) involves no free parameters. For the purpose of comparison, the CF parameters and the CF energy levels calculated from the simple point-charge model are also listed in the fifth column (column “PC”) of Table I and the fourth column of Table II. A brief description of the simple point-charge model is given in Appendix A.

The calculated CF parameter by the DFT may be divided into two parts. The first is calculated from the effective potential $V_{\text{eff}}(\mathbf{r})$ obtained directly from the DFT calculations and the second is from the repulsive pseudopotential $V_p(\mathbf{r})$ constructed from the DFT electron densities. The CF parameter values for these two parts are listed in the second and third columns (columns “DF” and “PP”) of Table I, respectively. It is shown that the calculated B_0^4 parameter of the DF part is too small compared to the fitted value in the last column and the B_0^6 parameter value is almost zero, which is

TABLE I. The CF parameters (in cm^{-1}) of Yb^{3+} in Cs_2NaYF_6 .

	DFT			PC	Fitted ^a
	DF	PP	Total		
B_0^4	482	1575	2057	367	1859
B_0^6	0.8	39.4	40.2	13	138

^aReference 8.

TABLE II. The CF energy levels (in cm^{-1}) of Yb^{3+} in Cs_2NaYF_6 .

$2S+1L_J$	IR	Energy levels			
		DFT	PC	Fitted ^a	Expt. ^a
$^2F_{7/2}$	Γ_6	0	0	0	0
	Γ_8	331	62	342	324
	Γ_7	850	153	782	656
$^2F_{5/2}$	Γ_8	10442	10283	10532	10389
	Γ_7	11031	10388	11062	11109

^aReference 8.

even smaller than that from the simple point-charge model (as listed in the fifth column). The main reason is that the overlap contribution to the CF parameters,⁹ which arises from the nonorthogonality between the all-electron $4f$ orbitals and the DFT-valence orbitals, has not been considered at this stage. By introducing a repulsive pseudopotential $V_p(\mathbf{r})$ to account for the orthogonal condition, as described in Sec. II B, the magnitudes are recovered, especially for the B_0^4 parameter. Moreover, a comparison of the DF and PP contributions to the B_0^4 and B_0^6 parameters reveals that the latter (overlap) contribution is predominant in the determination of both parameters. This large overlap contribution has the effect of repelling the $4f$ electrons from the ligand directions. This produces a CF contribution having the same sign as that produced by the negative F^- ions within the simple point-charge model. This is the case, as shown by a comparison of the parameter values in the third and fifth columns of Table I.

Because the $4f$ orbitals have been frozen in the core during the DFT calculations, the covalency contribution to the CF parameters, which arises from mixing of $4f$ and ligand wave functions and contributes to the crystal bonding, has been neglected. This contribution has the same sign as that of the overlap contribution⁹ and is expected to be small for the ionic $[\text{YbF}_6]^{3-}$ system. The covalency is particularly relevant to the B_0^6 parameter,²³ and hence the underestimation of the calculated B_0^6 parameter (40.2 cm^{-1}) with respect to the fitted one (138 cm^{-1}) may be presumably in part due to the neglect of covalency. It should be noted that the B_0^6 parameter is much less important than the B_0^4 in determining the CF energy-level splitting of Yb^{3+} in $\text{Cs}_2\text{NaYbF}_6$. The reason for this is twofold. The first is that the B_0^6 parameter is much smaller in magnitude than the B_0^4 parameter. The second is related to the relative magnitudes of the reduced matrix elements of the unit tensor operators U^k for $k=4, 6$. These reduced matrix elements are used in the angular part of the CF calculations. For $k=4$, $\langle ^2F_{2/5} \| U^4 \| ^2F_{2/5} \rangle = -0.67$ and $\langle ^2F_{2/7} \| U^4 \| ^2F_{2/7} \rangle = -0.86$, while for $k=6$, $\langle ^2F_{2/5} \| U^6 \| ^2F_{2/5} \rangle = 0$ and $\langle ^2F_{2/7} \| U^6 \| ^2F_{2/7} \rangle = -0.53$. The relative importance of the B_0^4 and B_0^6 parameters in the CF energy-level splitting has been illustrated for Yb^{3+} in $\text{Cs}_2\text{NaYbCl}_6$ in Ref. 8.

Besides the hybrid B3LYP exchange-correlation functional, the calculations have been performed using the “pure” PW91 (Refs. 24–26) and PBE (Ref. 27) generalized gradient approximation functionals. The results are listed in Table III.

TABLE III. The calculated CF parameters (in cm^{-1}) of Yb^{3+} in Cs_2NaYF_6 using the B3LYP, PW91, and PBE exchange-correlation functionals in the DFT calculations.

	B3LYP ^a			PW91			PBE		
	DF	PP	Total	DF	PP	Total	DF	PP	Total
B_0^4	482	1575	2057	508	1787	2295	505	1782	2287
B_0^6	0.8	39.4	40.2	0.5	39.6	40.1	0.4	39.3	39.7

^aThe results are identical to those in Table I.

One can see that the B_0^4 parameter value with the pure functionals is a little larger than that with the hybrid B3LYP functional. This is probably because the exchange effects of the DFT-valence electrons are better described by the hybrid B3LYP, where the exact Hartree-Fock exchange is partially mixed with the DFT exchange. The B_0^6 parameter is more sensitive to the exchange between the $4f$ and valence electrons.²³ However, the $4f$ electrons have been included in the core during the DFT calculations and thus the change of functionals makes no difference to the B_0^6 parameter.

The accuracy of our calculations mainly depends on that of the numerical integration in Eq. (7). Because the CF potential $V_{\text{CF}}(r, \theta, \varphi)$ in the vicinity of Yb^{3+} is highly nonuniform, as shown in Fig. 3, a fine grid mesh of $400 \times 400 \times 400$ integration points within a $4 \times 4 \times 4 \text{ \AA}^3$ cubic box centered on Yb^{3+} has been adopted. The radial $R_{4f}(r_i)$ at these integration points were obtained by interpolation of the radial wave function from the standard atomic calculation.²¹ The numerical accuracy can be roughly estimated. The B_q^k parameters with $k=2, 3, 5, 7$ and $q=-k, \dots, k$ ought to be zero due to the O_h site symmetry of Yb^{3+} in $\text{Cs}_2\text{NaYbF}_6$. Our calculations yield very small numbers for these CF parameters that are zero to two places of decimals. Moreover, the relations in Eq. (15) were very well reproduced by the numerical CF parameter values.

V. CONCLUSIONS

We have presented calculations of the CF parameters and energy levels for Yb^{3+} in the $\text{Cs}_2\text{NaYbF}_6$ crystal by a combination of the DFT with the conventional CFT. Our calculations are free of adjustable parameters. In the DFT calculations, the quasirelativistic ECP has been used for Yb^{3+} with the $4f$ shell frozen into the core. The CF potential constructed from the DFT can be divided into two parts. One is the DFT effective potential generated directly from DFT calculations. The other is a repulsive pseudopotential, which is constructed from the DFT electron densities to take into account the nonorthogonality between the $4f$ all-electron orbitals and the DFT-valence orbitals in the evaluation of the CF parameters. These parameters have been calculated by numerical integration, in which the numerical accuracy was ensured by adopting a fine grid mesh for the integration points. From the obtained parameters the CF energy levels have been calculated. The result is in good agreement with experiments. Furthermore, the calculated CF parameters have been discussed in terms of overlap, covalency, and ex-

change contributions for the $[\text{YbF}_6]^{3-}$ system, respectively. Especially, the overlap contribution is accounted for by the introduction of the repulsive pseudopotential. The contributions from covalency and exchange have also been addressed.

As discussed in the previous section, the agreement between the calculated and experimental CF energy levels of Yb^{3+} is partly due to the fact that the B_0^4 parameter is much more important than the B_0^6 in determining them. In cases where the B_0^6 is also important, for example, in crystals doped with Tm^{3+} and Er^{3+} , one cannot expect to obtain such an agreement in CF energy levels using the $4f$ -in-core ECP, because the covalency and exchange contributions associated with the $4f$ electrons, which are crucial to the B_0^6 parameter, are omitted. However, we emphasize that the B_0^4 parameter value can be predicted well by the present calculation procedure. Our preliminary studies on the $\text{Cs}_2\text{NaTmF}_6$ and $\text{Cs}_2\text{NaErF}_6$ crystals predict the B_0^4 to be 2105 and 2152 cm^{-1} , respectively, the latter being in good agreement with the experimental value of 2156 cm^{-1} .²⁸ To address the problem of the B_0^6 parameter, studies on the $\text{Cs}_2\text{NaLnF}_6$ systems, in which the $4f$ orbitals of lanthanide ions are included in the valence shell in the self-consistent DFT procedure, are in progress and will be discussed elsewhere.

ACKNOWLEDGMENTS

We wish to thank Ugo Cosentino, Università degli Studi di Milano-Bicocca, for the helpful discussion. The financial support from Fondazione CARIPLO-n.Prot.0018524 is acknowledged.

APPENDIX: THE CRYSTAL-FIELD PARAMETERS WITHIN THE SIMPLE POINT-CHARGE MODEL

In the conventional crystal-field theory, the electrostatic potential at point \mathbf{r} near a lanthanide ion may be expressed as a multipolar expansion centered on that ion,

$$V_{\text{CF}}(\mathbf{r}) = \int \frac{(-e)\rho(\mathbf{R})}{|\mathbf{R}-\mathbf{r}|} d\mathbf{R} = \sum_{k=0}^{\infty} \sum_{q=-k}^k A_q^k r^k c_q^k(\theta, \varphi), \quad (\text{A1})$$

where $\rho(\mathbf{R})$ represents any charge density distribution external to the point \mathbf{r} , e.g., the charge density of the ligand electrons and bare nuclei, and

$$A_q^k = \int \frac{(-e)\rho(\mathbf{R})}{R^{k+1}} C_q^{k*}(\Theta, \Phi) d\mathbf{R}. \quad (\text{A2})$$

Given that the one-electron $4f$ wave function can be factorized as a product of radial and angular parts, it is possible to replace Eq. (A1) by an expansion in which the radial integration has already been carried out, making the potential a function of the angular coordinates θ and φ alone. Equation (A1) can then be rewritten as

$$V_{\text{CF}}(\theta, \varphi) = \sum_{k=0}^{\infty} \sum_{q=-k}^k B_q^k C_q^k(\theta, \varphi), \quad (\text{A3})$$

where the crystal-field parameters

$$B_q^k = A_q^k \langle r^k \rangle. \quad (\text{A4})$$

Within the simple point-charge model,

$$\rho(\mathbf{R}) = \sum_{L=1}^N Ze \delta(\mathbf{R}_L - \mathbf{R}), \quad (\text{A5})$$

where Ze is the charge of ligand L at points \mathbf{R}_L . Substituting Eq. (A5) into Eq. (A2) yields

$$A_q^k = (-Ze^2) \sum_{L=1}^N \frac{1}{R_L^{k+1}} C_q^{k*}(\Theta_L, \Phi_L). \quad (\text{A6})$$

For the octahedral $[\text{YbF}_6]^{3-}$ complex with $N=6$ and $Z=-1$, it is shown, from Eq. (A6), that only A_q^k with $k=4, 6$, and $q=0, \pm 4$ are nonzero, and

$$A_0^4 = \frac{7}{2} \frac{e^2}{R^5}, \quad A_{\pm 4}^4 = (5/14)^{1/2} A_0^4,$$

$$A_0^6 = \frac{3}{4} \frac{e^2}{R^7}, \quad A_{\pm 4}^6 = -(7/2)^{1/2} A_0^6. \quad (\text{A7})$$

With $\langle r^4 \rangle = 1.085$ a.u. and $\langle r^6 \rangle = 1.085$ a.u., as obtained from the standard atomic calculations for Yb^{3+} ,²¹ and $R = 2.482 \text{ \AA}$,^{13,14} the crystal-field parameters in Eq. (A4) were calculated to be $B_0^4 = 367 \text{ cm}^{-1}$ and $B_0^6 = 13 \text{ cm}^{-1}$, as listed in the fifth column (column "PC") of Table I.

¹G. K. Liu, in *Spectroscopic Properties of Rare Earths in Optical Materials*, edited by G. K. Liu and B. Jacquier (Tsinghua University Press, Tsinghua, China, 2005), p. 1.

²M. Dolg, H. Stoll, and H. Preuss, *Theor. Chim. Acta* **85**, 441 (1993).

³D. Dai, L. Li, J. Ren, and M. H. Whangbo, *J. Chem. Phys.* **108**, 3479 (1998).

⁴J. Ren, M. H. Whangbo, D. Dai, and L. Li, *J. Chem. Phys.* **108**, 8479 (1998).

⁵U. Cosentino, A. Villa, D. Pitea, G. Moro, V. Barone, and A. Maiocchi, *J. Am. Chem. Soc.* **124**, 4901 (2002).

⁶X. Cao and M. Dolg, *Mol. Phys.* **101**, 2427 (2003).

⁷L. Smentek, J. B. A. Hess, J. P. Cross, H. C. Manning, and D. J. Bornhop, *J. Chem. Phys.* **123**, 244302 (2005).

⁸X. Zhou, M. D. Faucher, M. F. Reid, and P. A. Tanner, *J. Phys. Chem. B* **110**, 14939 (2006).

⁹D. J. Newman and B. Ng, in *Crystal Field Handbook*, edited by D. J. Newman and B. Ng (Cambridge University Press, Cambridge, UK, 2000), p. 6.

¹⁰W. Kohn and L. J. Sham, *Phys. Rev.* **140**, A1133 (1965).

¹¹J. Kohanoff, *Electronic Structure Calculations for Solids and Molecules: Theory and Computational Methods* (Cambridge University Press, Cambridge, UK, 2006), pp. 143–177.

¹²L. Szasz, *Pseudopotential Theory of Atoms and Molecules* (Wiley, New York, 1985).

¹³E. Bucher, H. J. Guggenheim, K. Andres, G. W. Hull, and A. S. Cooper, *Phys. Rev. B* **10**, 2945 (1974).

¹⁴G. Meyer, *Prog. Solid State Chem.* **14**, 141 (1982).

¹⁵A. D. Becke, *J. Chem. Phys.* **98**, 5648 (1993).

¹⁶C. Lee, W. Yang, and R. G. Parr, *Phys. Rev. B* **37**, 785 (1988).

¹⁷M. J. Frisch, *et al.*, GAUSSIAN03, Revision B.04, Gaussian, Inc., Pittsburgh, PA, 2003.

¹⁸M. Dolg, H. Stoll, A. Savin, and H. Preuss, *Theor. Chim. Acta* **75**, 173 (1989).

¹⁹M. Dolg, H. Stoll, and H. Preuss, *J. Chem. Phys.* **90**, 1730 (1989).

²⁰S. Edvardsson and D. Åberg, *Comput. Phys. Commun.* **133**, 396 (2001).

²¹R. D. Cowan, *The Theory of Atomic Structure and Spectra* (University of California, Berkeley, 1981).

²²W. T. Carnall, G. L. Goodman, K. Rajnak, and R. S. Rana, *J. Chem. Phys.* **90**, 3443 (1989).

²³M. M. Ellis and D. J. Newmann, *J. Chem. Phys.* **47**, 1986 (1967).

²⁴J. P. Perdew and Y. Wang, *Phys. Rev. B* **33**, 8800 (1986).

²⁵J. P. Perdew, J. A. Chevary, S. H. Vosko, K. A. Jackson, M. R. Pederson, D. J. Singh, and C. Fiolhais, *Phys. Rev. B* **46**, 6671 (1992).

²⁶J. P. Perdew, J. A. Chevary, S. H. Vosko, K. A. Jackson, M. R. Pederson, D. J. Singh, and C. Fiolhais, *Phys. Rev. B* **48**, 4978 (1993).

²⁷J. P. Perdew, K. Burke, and M. Ernzerhof, *Phys. Rev. Lett.* **77**, 3865 (1996).

²⁸X. Zhou, P. A. Tanner, and M. D. Faucher, *J. Phys. Chem. C* **111**, 683 (2007).